Substituent effects on silene reactivity — Reactive silenes from photolysis of phenylated tri- and tetrasilanes

William J. Leigh,[1] Andrey G. Moiseev, Eugenie Coulais, Farahnaz Lollmahomed, and Mohammad S. Askari

Abstract: Laser flash photolysis of 2-phenylheptamethyltrisilane (**5d**), 2,2-diphenylhexamethyltrisilane (**5e**), and phenyltris(trimethylsilyl)silane (**5f**) in hexane and acetonitrile solution affords strong, long-lived transient absorptions centered in the 440–470 nm range, which are assigned to the transient silenes formed via [1,3]-trimethylsilyl migration into the ortho-position of a phenyl ring on the basis of their UV–vis spectra and kinetic data for their reactions with methanol (MeOH), acetic acid (AcOH), acetone, 2,3-dimethyl-1,3-butadiene (DMB), carbon tetrachloride (CCl_4), and oxygen. The silene derivatives are formed along with the corresponding silylenes ($SiMePh$, $SiPh_2$, and $Si(SiMe_3)Ph$, respectively) upon photolysis of these compounds in solution, and indeed, weak, short-lived transient absorptions assignable to the silylenes can also be detected in laser photolysis experiments with the three compounds in hexane, superimposed on the much more prominent absorptions due to the silenes. The silylene absorptions are quenched by MeOH and triethylsilane (Et_3SiH) with absolute rate constants varying over the narrow ranges of $(1.1–1.8) \times 10^{10}$ $(mol/L)^{-1}$ s^{-1} and $(2.5–3.6) \times 10^9$ $(mol/L)^{-1}$ s^{-1}, respectively, in excellent agreement with previously reported values for $SiPh_2$ and $SiMe_2$ under the same conditions. The kinetic data obtained for the silenes are compared to previously reported data for the reactions of the same substrates with the related silenes (**6a–6c**) formed by photolysis of pentamethylphenyl-, 1,1,1,2-tetramethyl-2,2-diphenyl-, and 1,1,1-trimethyl-2,2,2-triphenyldisilane (**5a–5c**, respectively) under similar conditions. The comparison provides the first systematic, quantitative assessment of the stabilizing effects of trialkylsilyl substitution at the silenic silicon atom in silene derivatives.

Key words: silene, silylene, trisilane, tetrasilane, kinetics.

Résumé : La photolyse éclair au laser du 2-phénylheptaméthyltrisilane (**5d**), du 2,2-diphénylhexaméthyltrisilane (**5e**) et du phényltris(triméthylsilyl)silane (**5f**), en solution dans l'hexane et l'acétonitrile, permet d'observer de fortes absorptions transitoires de longue durée, centrées autour de 440 à 470 nm et qui, sur la base de leurs spectres UV/vis et des données cinétiques de leurs réactions avec le méthanol (MeOH), l'acide acétique (AcOH), l'acétone, le 2,3-diméthyl-1,3-butadiène (DMB), le tétrachlorure de carbone (CC_4) et l'oxygène, ont été attribuées aux silènes transitoires formés par le biais d'une migration [1,3]-triméthylsilyle vers la postion ortho d'un noyau phényle. Lors de la photolyse des ces composés en solutions, les dérivés silènes se forment aux côtés des silylènes correspondants [respectivement ($SiMePh$, $SiPh_2$ et $Si(SiMe_3)Ph$] et, dans les expériences de photolyse laser des trois composés en solution dans l'hexane, on peut de fait détecter des absorptions transitoires de courtes durées attribuables aux silylènes qui sont superposées sur les absorptions beaucoup plus prééminentes dues aux silènes. Les absorptions des silylènes peuvent être piégées par le méthanol et le triéthylsilane (Et_3SiH), avec des constantes de vitesse absolues qui s'étalent respectivement sur une plage étroite allant de $(1,1–1,8) \times 10^{10}$ $(mol/L)^{-1}$ s^{-1} à $(2,5–3,6) \times 10^{10}$ $(mol/L)^{-1}$ s^{-1}, en excellent accord avec les valeurs rapportées antérieurement pour le $SiPh_2$ et le $SiMe_2$, dans les mêmes conditions. On compare les données cinétiques obtenues pour les silènes avec celles obtenues antérieurement pour les réactions des mêmes substrats avec les silènes apparentés, **6a–6c**, formés par photolyse des pentaméthylphényl-, 1,1,1,2-tétraméthyl-2,2-diphényl- et 1,1,1-triméthyl-2,2,2-triphényldisilanes (**5a–5c**, respectivement), dans des conditions similaires. La comparaison fournit la première évaluation systématique et quantitative des effets stabilisants de la substitution par un groupement trialkylsilyle au niveau de l'atome de silicium silénique dans les dérivés silènes.

Mots-clés : silène, silylène, trisilane, tétrasilane, cinétique.

[Traduit par la Rédaction]

W.J. Leigh,[1] A.G. Moiseev, E. Coulais, F. Lollmahomed, and M. Askari. Department of Chemistry, McMaster University, 1280 Main Street West, Hamilton, ON L8S 4M1, Canada.

[1]Corresponding author (e-mail: leigh@mcmaster.ca).

Introduction

The Si=C double bond is an intrinsically reactive bonding arrangement that has received a great deal of theoretical and experimental attention over the past few decades (1–4). Most silenes are transients in solution or the gas phase, reacting rapidly with nucleophiles or oxygen, or by dimerization when reactive substrates are absent. Successful attempts to synthesize isolable silene derivatives have invariably relied on the presence of sterically bulky substituents to suppress dimerization, which in most cases proceeds via formal head-to-tail [2+2] cycloaddition. This purely kinetic stabilizing effect has also been supplemented with thermodynamic stabilization, most notably with the introduction of trialkylsilyl substituents at the silenic silicon atom and alkyl- and (or) alkoxy-substituents at carbon, such as in the well-known silenes of Brook (**1** (5)) and Apeloig (**2** (6)) and their co-workers. It is well established that such substitution patterns lead to marked reductions in the natural ($^{\delta+}$Si=C$^{\delta-}$) polarity associated with the Si=C double bond, slowing the normally diffusion-controlled dimerization reaction (7, 8) and reversing its normal (head-to-tail) regiochemistry (6, 9) (Chart 1).

While an abundance of evidence suggests that, by and large, weakly polar silenes such as **1** and **2** display similar reactivity as do more polar derivatives toward most substrates in terms of reaction products, relatively few studies have been carried out with the aim of quantifying the effects of reduced Si=C bond polarity on reaction kinetics or mechanisms. Our group has studied the kinetics of the reaction of **2** and a sterically stabilized derivative with methanol (MeOH) in hexane solution, and found that not only does this silene derivative react several orders of magnitude more slowly with the alcohol than do other transient silenes that have been studied, it reacts via a different mechanism (8). The results (both experimental and computational) are consistent with a concerted mechanism involving reaction of the hydrogen-bonded dimer of the alcohol in hexane solution, in contrast to the two-step mechanism, initiated by nucleophilic attack at silicon followed by proton transfer to carbon, which is typical of more electrophilic, naturally polarized transient silenes such as 1,1-diphenylsilene (**3**) (3, 10, 11). Milnes and Baines (12) have recently reported a mechanistic probe study of the effects of Si=C bond polarity on the mechanism of the reaction of two kinetically stabilized silenes with aldehydes, and have shown it to change from one involving a zwitterionic intermediate in the case of the naturally polarized silene **4** to a biradical pathway in the case of the very weakly polar Brook silene **1** (R = *t*-butyl or adamantyl) (Chart 2).

Some time ago, we reported two experimental studies directed at quantifying the effects of substituents at silicon and carbon on the kinetics of nucleophilic additions to transient silenes (13, 14). Though systematic, these studies were limited to alcohol additions, and furthermore, covered only silenes of the general structure Me(R)Si=CH$_2$ and Me$_2$Si=CHR. We have continued to search for opportunities to extend the scope of these studies to include both mono- and bis-SiMe$_3$ substitution at the silenic silicon atom and to examine the effects of these substituents on other aspects of
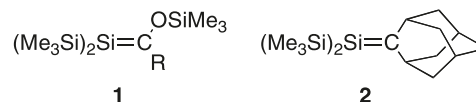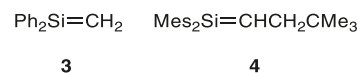
Chart 1.

Chart 2.

Scheme 1.

a. $R_1 = R_2 = Me$
b. $R_1 = Me; R_2 = Ph$
c. $R_1 = R_2 = Ph$
d. $R_1 = Me; R_2 = SiMe_3$
e. $R_1 = Ph; R_2 = SiMe_3$
f. $R_1 = R_2 = SiMe_3$

silene reactivity, in addition to nucleophilic addition reactions, in as systematic a manner as possible.

It occurred to us that just such an opportunity presents itself with the series of 1-silahexatriene derivatives, **6a–6f**, which are derived from the corresponding oligosilanes, **5a–5f**, by photochemical [1,3]-trimethylsilyl migration (Scheme 1). The first three members of the series (**6a–6c**) have been studied by us previously by laser photolysis methods (15–17), and so a considerable body of kinetic data already exists for these compounds. The last three members of the series (**6d–6f**) are known to be formed as coproducts in the photolysis of the tri- and tetrasilanes, **5d–5f**, which are better known as photochemical precursors of the transient *silylene* derivatives SiPh$_2$, SiMePh, and Si(Ph)SiMe$_3$, respectively (18–22). Photolysis of these compounds in solution is known to afford the corresponding silylenes in chemical yields of 40%–60%, from the results of trapping studies in which the silylenes of primary interest were scavenged with substrates such as alkenes, dienes, ketones, trialkylsilanes, and alcohols. *Some* of these studies also reported significant yields of products derived from trapping of the transient 1-silahexatriene derivatives, **6d–6f**, in chemical yields as high as ca. 40% (18, 23–30). Gaspar and co-workers employed **5d** and **5e** as precursors to SiMePh (31, 32) and SiPh$_2$ (33), respectively, in some of the earliest reported attempts to study reactive silylenes in solution by laser flash photolysis methods. They described strongly absorbing, long-lived transient species that they assigned (with some reservation) to the corresponding silylenes (31–33); however, as we have recently shown in the case of **5e** (34), it is more likely that the species they characterized in their experiments are in fact the corresponding 1-silahexatriene derivatives and not the silylenes of interest.

The course of the reactions of silenes of this type with typical "silenophiles" is often different than that found with most other silenes, owing to the fact that the silenic carbon is part of a carbocyclic ring system containing both an allylic hydrogen and a dienyl moiety in conjugation with the Si=C bond. For example, aliphatic dienes and alkenes react with these silenes via ene-addition rather than by the usual

[4+2] or [2+2] cycloaddition pathways that are typical of most other silene derivatives (1, 2, 18, 35); these reactions are diverted from their normal course by the labile allylic hydrogen, whose transfer to a carbon in the substrate results in aromatization of the carbocyclic ring. Reaction with acetone proceeds via competing [2+2] and ene-addition (30, 36–38), the latter again involving transfer of the allylic hydrogen in the silene to the substrate rather than via the usual pathway (as exemplified by **3** (39)) to produce a silyl enol ether. Finally, the presence of the cyclohexadienyl-substituent in silenes of this type results in unusually high reactivity toward molecular oxygen and CCl_4, which are thought to react via mechanisms involving radical or biradical intermediates (16).

In the present paper, we report the results of a laser flash photolysis study of **5d**–**5f** in various solvents. As suggested above, the main goal of the work was to establish that the 1-silahexatriene derivatives are the dominant transient products detectable in experiments of this type with these compounds, to characterize their reactivities with a variety of substrates that show characteristically high reactivity toward silenes of this type, and to compare the results to previously published data for the related silenes **6a**–**6c** in the interest of elaborating on our understanding of substituent effects on various aspects of silene reactivity. A secondary goal was to attempt to detect the reactive silylenes SiMePh and Si(Ph)SiMe$_3$ in solution by laser photolysis of **5d** and **5f**, to provide a benchmark for future studies with potentially more appropriate photochemical precursors to these silylene derivatives; to our knowledge, **5f** has not been studied previously by laser photolysis methods.

Results

Laser flash photolysis of rapidly flowed solutions of 2-phenylheptamethyltrisilane (**5d**; ~10^{-4} mol/L) in dry, deoxygenated hexane, with the pulses from a KrF excimer laser (248 nm; ~20 ns; ~100 mJ) afforded strong transient absorptions centered at λ_{max} = 440 nm, which decay over several hundred microseconds with multiexponential kinetics, in good agreement with the results of earlier flash photolysis studies of this compound (31, 32). We assign this absorption to silene **6d** based on the similarity of its spectrum to those of **6e** (λ_{max} = 460 nm (34)) and **6a**–**6c** (λ_{max}= 425–490 nm (16, 17)), and the kinetic evidence described later in the paper. However, we also detected a second, much shorter-lived transient absorption that was superimposed on those due to the long-lived species and exhibited a lifetime τ ~ 3 μs. The species exhibited a distinct absorption band centered at λ_{max} ~ 270 nm and weaker absorptions throughout the 400–600 nm range. Figure 1 shows representative transient spectra, recorded 128–256 ns and 4.86–5.09 μs after the laser pulse, along with decay traces recorded at 440 nm and 510 nm. As in our previous study of **5e** (34), addition of 3 mmol/L Et$_3$SiH reduced the lifetime of the short-lived species to ca. 100 ns without affecting the lifetime of the strong 440 nm absorption, thus cleaning up the 128–256 ns spectrum considerably (see Fig. 1b). We also recorded a UV–vis spectrum of a photolysed solution of **5d** in 3-methylpentane (MP) at 78 K, which is shown as the solid
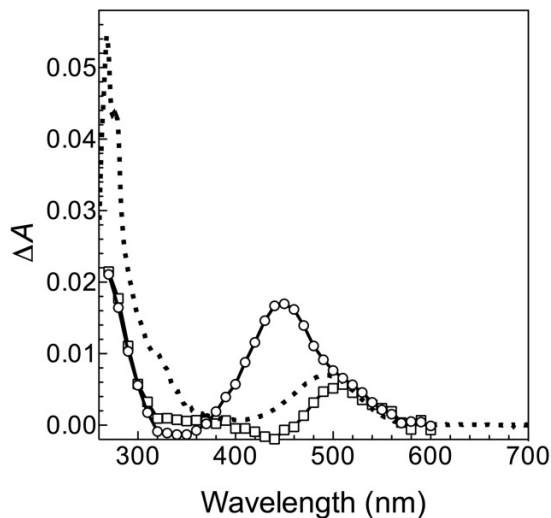
Fig. 1. Transient absorption spectra recorded 128–256 ns (-○-) and 4.86–5.09 μs (-□-) after the laser pulse, from the laser flash photolysis of 0.11 mmol/L solutions of 2-phenylheptamethyl-trisilane (**5d**) in (*a*) hexane and (*b*) hexane containing 3.0 mmol/L Et$_3$SiH. The insets show transient decays recorded at 440 and 510 nm. The spectrum obtained from a photolysed solution of **5d** in 3-methylpentane at 78 K (—; scaled to match the absorption intensities below 310 nm) is also shown in (*a*).
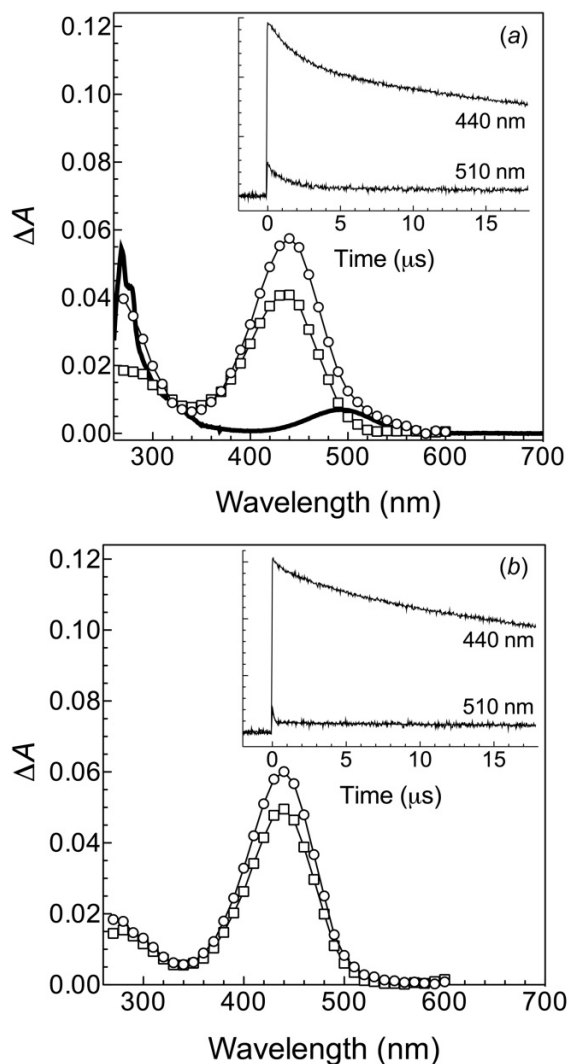
line in Fig. 1. The low temperature matrix spectrum (λ_{max} = 268, 493 nm) agrees well with that reported by West and coworkers (40), who assigned it to methylphenylsilylene (SiMePh).

The low temperature spectrum is reproduced again in Fig. 2, along with solution phase difference spectra calculated from the spectra of Fig. 1 in two ways. The first spectrum (-□-) was calculated as the difference between the end-of-pulse (128–256 ns) spectra in pure hexane (Fig. 1a) and in hexane containing 3 mmol/L Et$_3$SiH (Fig. 1b), and thus isolates that portion of the end-of-pulse spectrum that is quenched by a primary reaction with the silane. Clearly, the difference spectrum (λ_{max} = 270, 510 nm) agrees with the matrix spectrum of SiMePh quite closely; it is also quite similar to the reported solution phase and low temperature

Fig. 2. Transient difference spectra, calculated as the difference between the 128–256 ns spectrum of Fig. 1a minus the 128–256 ns spectrum of Fig. 1b (-□-), and as the difference between the 128–256 ns and 4.86–5.09 μs spectra of Fig. 1a (-○-). The dashed line is the spectrum recorded of a photolysed solution of **5d** in 3-methylpentane at 78 K, reproduced from Fig. 1a.
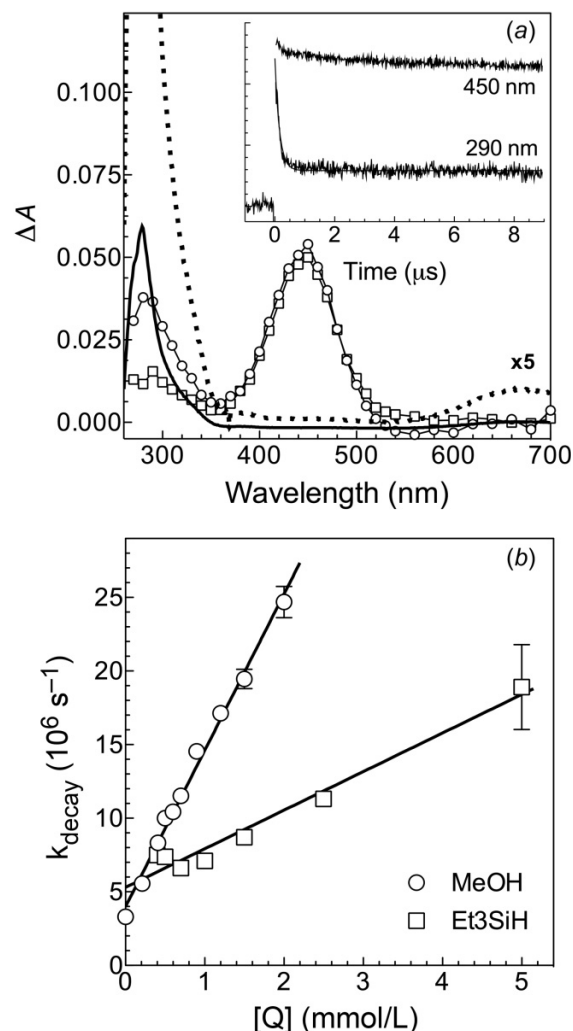

Fig. 3. (a) Transient absorption spectra recorded 16–80 ns (-○-) and 432–544 ns (-□-) after the laser pulse, from the laser photolysis of a 0.07 mmol/L solution of phenyltris(trimethyl-silyl)silane (**5f**) in deoxygenated hexane, and the scaled spectrum of a photolysed solution of **5f** in 3-methylpentane at 78 K (—); the dotted line shows the latter spectrum magnified by a factor of 5. The inset shows transient decays recorded at 290 and 450 nm. (b) Plots of k_{decay} vs [Q] for quenching of the short-lived transient ($\lambda_{max} \sim 285$ nm) from **5f** by MeOH (○) and Et$_3$SiH (□) in deoxygenated hexane at 25 °C; the solid lines are the linear least-squares fits of the data to eq. [1].

matrix spectra of SiPh$_2$ (34, 40). We thus assign the short-lived absorptions centered at 270 and 510 nm to the silylene, SiMePh. Further support for the assignment is provided by the second order rate constants for quenching of the species by MeOH ($k_{MeOH} = (1.8 \pm 0.3) \times 10^{10}$ (mol/L)$^{-1}$ s^{-1}), Et$_3$SiH ($k_{Et_3SiH} = (3.4 \pm 0.3) \times 10^9$ (mol/L)$^{-1}$ s^{-1}), and molecular oxygen ($k_{O_2} = (1.8 \pm 0.2) \times 10^8$ (mol/L)$^{-1}$ s^{-1}), which were determined from (linear) plots of the pseudo first-order rate constant for decay of the transient signal at 520 nm versus substrate (Q) concentration according to eq. [1]. The rate constants are quite similar to those for the reaction of SiMe$_2$ and SiPh$_2$ with these three substrates in hexane under similar conditions (41); furthermore, the ratio of the absolute rate constants for quenching of the species by MeOH and Et$_3$SiH ($k_{MeOH}/k_{Et_3SiH} = 5.3 \pm 1.5$) are quite close to the rate ratio determined by Hawari et al. (42) from the competitive trapping of SiMePh by ethanol and Et$_3$SiH in cyclohexane ($k_{EtOH}/k_{Et_3SiH} = 4.8$). The lifetime of the 440 nm absorption in the presence of millimolar concentrations of MeOH and Et$_3$SiH was roughly the same as in pure hexane solution, consistent with its assignment to silene **6d**.

[1] $k_{decay} = k_0 + k_Q[Q]$

The second spectrum of Fig. 2 (-○-) was calculated as the difference between the end-of-pulse and 4.9–5.1 μs spectra of Fig. 1a, and thus isolates that portion of the 128–256 ns spectrum of Fig. 1a that decays in the first 5 μs after excitation in pure hexane solution (i.e., in the absence of a silylene scavenger). This difference spectrum clearly contains contributions from both SiMePh and silene **6d**, consistent with the presence of a fast initial decay process for the silene that exists only in the absence of a silylene scavenger. We tentatively identify this process as a bimolecular reaction of the silene and silylene; comparison of the maximum absorbance values of the early and late spectra of Figs. 1a and 1b indicate that roughly 20% of the initially produced amount of **6d**

undergoes this rapid initial decay process. No evidence for the formation of the silylene dimerization product, 1,2-dimethyl-1,2-diphenyldisilene (Si$_2$Me$_2$Ph$_2$; $\lambda_{max} = 420$ nm (43)), could be obtained in any of these experiments, consistent with its formation being quenched as a result of the competing reaction of SiMePh with silene **6d**.

Similarly, laser flash photolysis of a rapidly flowed 7 × 10^{-5} mol/L solution of phenyltris(trimethylsilyl)silane (**5f**) in hexane afforded a transient spectrum consisting of two main components, one very long-lived one centered at $\lambda_{max} = 450$ nm, which decayed over several milliseconds with mixed order kinetics, and one very short-lived one centered at $\lambda_{max} \sim 285$ nm that decayed with first order kinetics and

Table 1. Absolute rate constants (units of 10^6 (mol/L)$^{-1}$s^{-1}, unless otherwise noted) for the quenching of silenes **6a**–**6f** by various substrates in hydrocarbon solvents and MeCN at 25 °C.

Substrate	**6a**	**6b**	**6c**	**6d**	**6e**	**6f**
λ_{max}	425 nm	460 nm	490 nm	440 nm	460 nm	450 nm
MeOH[a]	$k_1 = 230 \pm 70$[b]	$k_1 = 60 \pm 25$[b]	$k_1 = 17 \pm 10$[b]	$k_2 = 2.47 \pm 0.03$[c]	$k_2 = 0.80 \pm 0.01$[c]	$\tau_{MeOH} \sim 38$ μs
	$k_2 = 4900 \pm 1000$[b,c]	$k_2 = 2800 \pm 500$[b,c]	$k_2 = 1100 \pm 400$[b,c]			
AcOH[a]	290 ± 10[b]	141 ± 5[b]	70 ± 2[b]	11.7 ± 0.3	2.7 ± 0.1	0.025 ± 0.001
Acetone	4500 ± 60[d]	1580 ± 60[d]	542 ± 5[d]	4.3 ± 0.1	1.9 ± 0.1	0.09 ± 0.01
DMB	128 ± 3[d]	68 ± 1[d]	30 ± 1[d]	0.11 ± 0.006[e]	0.083 ± 0.003[e]	0.011 ± 0.006
CCl$_4$	440 ± 10[d]	160 ± 10[d]	110 ± 10[d]	78 ± 2	23 ± 1	4.9 ± 0.2
O$_2$	690 ± 40[d]	350 ± 10[d]	190 ± 20[d]	120 ± 5	39 ± 2	11.4 ± 0.2

Note: In hexane solution unless otherwise noted.
[a]In MeCN solution, see eq. [2].
[b]Data from ref. 17.
[c]In units of 10^6 (mol/L)$^{-2}$ s^{-1}.
[d]In isooctane solution, data from ref. 16.
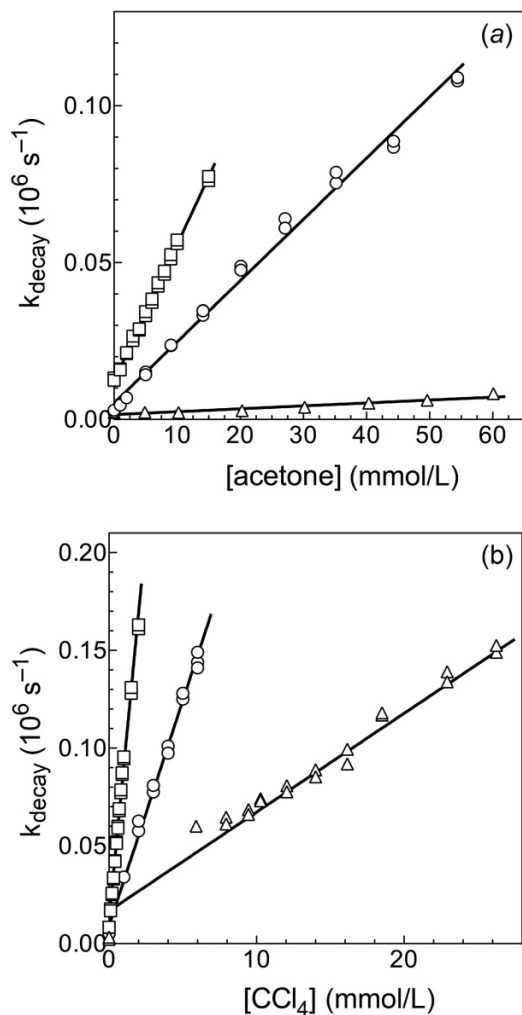[e]In cyclohexane solution, data from refs. 31 and 33.

lifetime $\tau \sim 300$ ns. Figure 3a shows transient spectra recorded 16–80 and 432–544 ns after the laser pulse, along with the UV–vis spectrum of a photolysed sample of **5f** in a 3-MP matrix at 78 K. The matrix spectrum ($\lambda_{max} = 280$, 680 nm) agrees well with the one reported by Conlin and co-workers, who assigned it to phenyltrimethylsilylsilylene (Si(Ph)SiMe$_3$) (44). The lifetime of the transient signal at 290 nm was shortened upon addition of MeOH or Et$_3$SiH to the solution. Plots of k_{decay} versus [Q] were linear, analysis of which, according to eq. [1], afforded the second order rate constants $k_{MeOH} = (1.1 \pm 0.1) \times 10^{10}$ (mol/L)$^{-1}$ s^{-1} and $k_{Et_3SiH} = (2.6 \pm 0.4) \times 10^9$ (mol/L)$^{-1}$ s^{-1} for reaction of the species with MeOH and Et$_3$SiH, respectively. These results are consistent with the assignment of the short-lived 285 nm absorption band to Si(Ph)SiMe$_3$. Unfortunately, the presence of the weak long wavelength band, which is observable in the matrix spectrum, could not be detected in solution, due undoubtedly to the much lower extinction coefficient of this absorption relative to that at 285 nm, which is itself relatively weak. The lifetime of the 450 nm transient was unaffected in the presence of the millimolar quantities of MeOH and Et$_3$SiH that were required to effect a change in the lifetime of the 285 nm absorption, allowing preliminary assignment of the 450 nm absorption to silene **6f**.

Laser photolysis of solutions of **5e** ($\sim 10^{-4}$ mol/L) in deoxygenated hexane afforded similar results to those reported in our preliminary study of this compound (45): two distinct transient species are formed, one that exhibits $\lambda_{max} = 460$ nm and decays over several milliseconds, and one that exhibits a discrete absorption band at $\lambda_{max} = 290$ nm, weaker absorptions in the 490–530 nm range and decays over 1–2 μs. The latter is quenched efficiently by added MeOH ($k_{MeOH} = (1.32 \pm 0.04) \times 10^{10}$ (mol/L)$^{-1}$ s^{-1}) and Et$_3$SiH ($k_{Et_3SiH} = (3.5 \pm 0.2) \times 10^9$ (mol/L)$^{-1}$ s^{-1}), consistent with a silylene (SiPh$_2$) assignment (34). Again, the lifetime of the long-lived species is unaffected by these reagents in millimolar concentrations (34).

Addition of acetone or carbon tetrachloride (CCl$_4$) to the hexane solutions of **5d**–**5f** caused the decay of the silene absorptions to accelerate in proportion to substrate concentration and follow clean pseudo first kinetics. Plots of k_{decay} versus [Q] were linear, and were analyzed according to eq. [1] to obtain the second order rate constants listed in Table 1. Figure 4 shows representative plots of k_{decay} versus [Q] for quenching of silenes **6d**–**6f** by acetone and CCl$_4$. The lifetimes of the silenes were also observed to decrease upon addition of oxygen to the solutions; second-order quenching rate constants were estimated from three-point plots of k_{decay} values recorded in argon-, air-, and O$_2$-saturated solutions of **5d**–**5f** in hexane versus [O$_2$], which exhibited good linearity in all three cases. Addition of up to 10 mmol/L 2,3-dimethyl-1,3-butadiene (DMB) to hexane solutions of **5f** had little effect on the intensity or lifetime of the 450 nm signal due to silene **6f**, as expected considering the reported rate constants for reaction of the long-lived transients from **5d** and **5e** (i.e., silenes **6d** and **6e**) with this diene, which are in the range of ca. 10^5 (mol/L)$^{-1}$ s^{-1} in cyclohexane (31, 33). Addition of larger quantities of the diene (30–40 mmol/L) led to corresponding reductions in the intensity of the silene absorption due to screening of the excitation light by the added substrate, and very modest increases in the pseudo first order decay rate constant. A plot of k_{decay} versus [DMB] was linear over the 30–40 mmol/L range in added diene, and afforded an estimate of $k_{DMB} = (1.1 \pm 0.1) \times 10^4$ (mol/L)$^{-1}$ s^{-1} for the second order rate constant for reaction of DMB with **6f**.
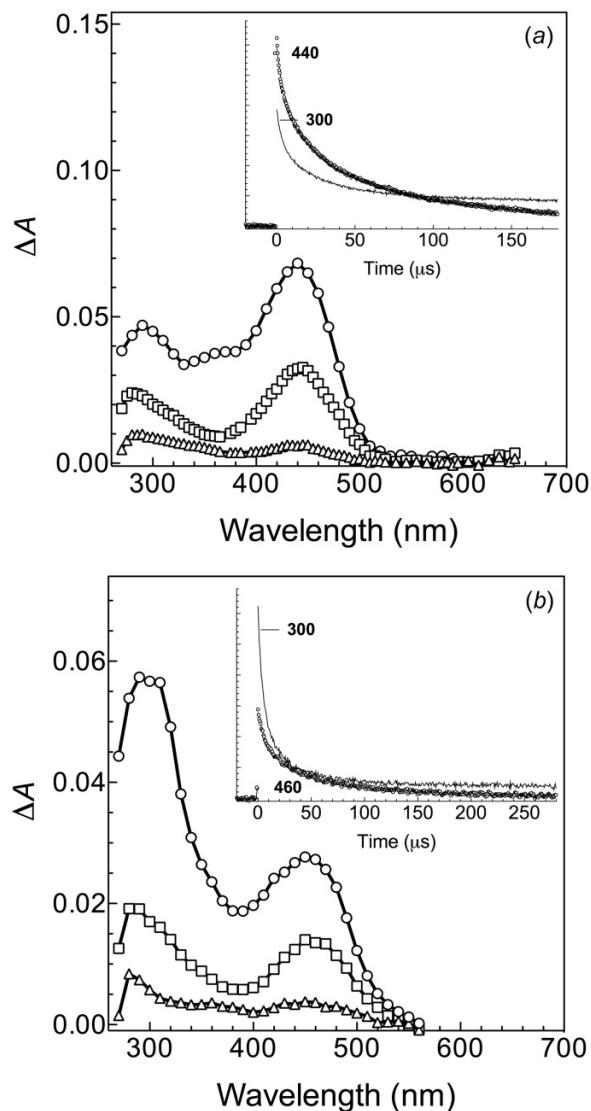
Quenching of the three silenes by methanol (MeOH) and acetic acid (AcOH) was studied in acetonitrile (MeCN) solution, as preliminary experiments indicated that the effects of these substrates on the silene lifetimes were too small for meaningful rate constants to be determined in hexane, given the solubility limits of the two substrates in the hydrocarbon solvent. Laser photolysis of **5d**–**5f** in deoxygenated MeCN led in each case to the formation of two long-lived transient

Fig. 4. Plots of k_{decay} vs [Q] for the quenching of silenes **6d** (□), **6e** (○), and **6f** (△) by (*a*) acetone and (*b*) CCl$_4$ in deoxygenated hexane at 25 °C. The solid lines are the linear least-squares fits of the data to eq. [1].

Fig. 5. (*a*) Transient absorption spectra recorded 32–96 ns (-○-), 13.1–13.8 μs (-□-), and 139.5–140.6 μs (△) after the laser pulse, from the laser photolysis of a 0.07 mmol/L solution of **5d** in deoxygenated MeCN; the inset shows transient decays recorded at 300 and 440 nm. (*b*) Transient absorption spectra recorded 0–1.2 μs (-○-), 15.4–16.6 μs (-□-), and 99.8–101.1 μs (△) after the laser pulse, from the laser photolysis of a 0.07 mmol/L solution of **5e** in deoxygenated MeCN; the inset shows transient decays recorded at 300 and 460 nm.

species, one exhibiting an absorption maximum in the 440–460 nm range and a lifetime similar to that of the corresponding transient in hexane and hence assignable to the corresponding silenes, and the second exhibiting λ_{max} ~ 310 nm. The latter absorptions decayed on a distinctly faster time scale with both **5d** and **5e**, but on a similar time scale to the 450 nm absorption in the case of **5f**. Transient absorption spectra recorded at various times after the laser pulse for **5d** and **5e** in MeCN are shown in Fig. 5, while the analogous spectra obtained with **5f** are shown in Fig. 6*a*. Addition of MeOH to the MeCN solutions of **5d** and **5e** caused the lifetimes at 450 nm to shorten and the decays to follow clean pseudo first order kinetics. As we anticipated based on our earlier studies of silenes **6a–6c** (16, 17), plots of k_{decay} versus [MeOH] exhibited positive curvature; polynomial least-squares fitting of the data to eq. [2] revealed a good correlation with the square of the MeOH concentration, as is illustrated in Fig. 7*a*. In contrast, the lifetime of silene **6f** in MeCN was barely affected upon addition of up to ca. 2 mol/L MeOH, so no attempt was made to determine a rate

constant in this case. Silene **6f** could actually be detected quite easily in neat MeOH solution, where it exhibited a lifetime of τ ~ 38 μs and the same absorption maximum as in hexane and MeCN; the spectrum is shown in Fig. 6*b*. The effect of added MeOH on the short wavelength signals observed in experiments in MeCN solution was not investigated.

[2] $k_{decay} = k_0 + k_1[MeOH] + k_2[MeOH]^2$

In contrast to the behavior observed with MeOH, addition of AcOH to MeCN solutions of **5d–5f** resulted in increases in k_{decay} that varied linearly with concentration in all three

Fig. 6. (*a*) Transient absorption spectra recorded 0–3.2 μs (-○-), 57.6–60.8 μs (-□-), and 540–542 μs (Δ) after the laser pulse, from the laser photolysis of a 0.07 mmol/L solution of **5f** in deoxygenated MeCN; the inset sh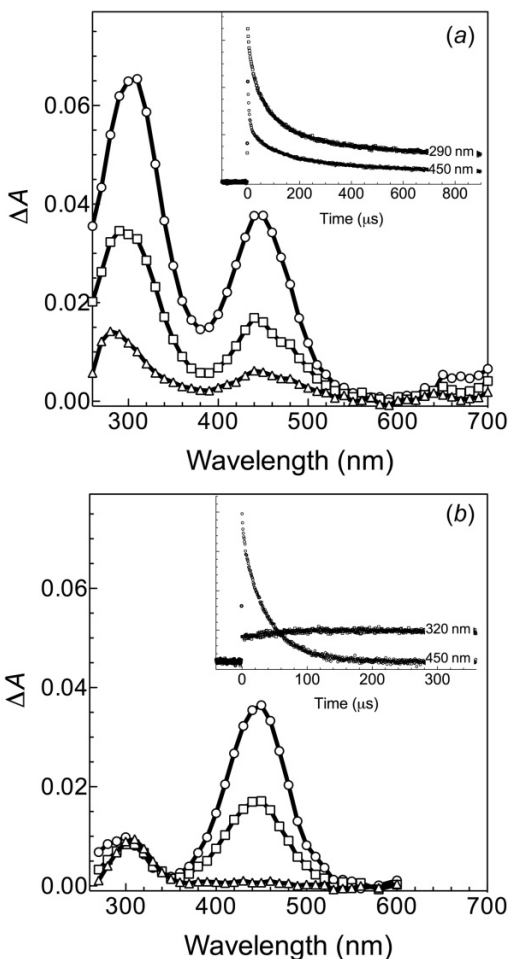ows transient decays recorded at 290 and 450 nm. (*b*) Transient absorption spectra recorded 0–0.6 μs (-○-), 23.0–24.3 μs (-□-), and 135–136 μs (Δ) after the laser pulse, from the laser photolysis of a 0.07 mmol/L solution of **5f** in deoxygenated MeOH; the inset shows transient decays recorded at 320 and 450 nm.
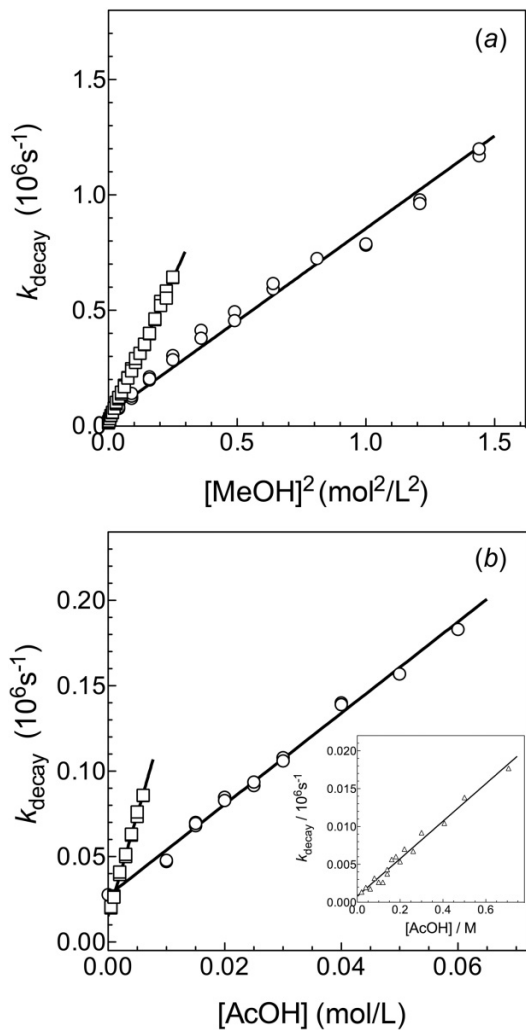

Fig. 7. Plots of (*a*) k_{decay} vs $[MeOH]^2$ and (*b*) k_{decay} vs [AcOH] for the quenching of silenes **6d** (□) and **6e** (○) by MeOH and AcOH in deoxygenated MeCN at 25 °C; the inset in (*b*) shows the quenching plot for silene **6f** by AcOH.

cases. The corresponding quenching plots are shown in Fig. 7*b*.

The kinetic data obtained in these experiments are summarized in Table 1, along with the corresponding, previously reported data for **6a**–**6c**.

Discussion

While early product studies of the photochemistry of **5d**–**5f** focused largely on the reactions of the corresponding silylenes (SiMePh, SiPh$_2$, and Si(Ph)SiMe$_3$, respectively) with various substrates (18, 19, 21, 22), several of them also reported the isolation of products derived from trapping of silenes **6d**–**6f**; specifically, those studies that employed aliphatic dienes (23, 26, 37), terminal alkenes (29, 30), acetone (37), or alcohols (24, 25, 27) as trapping agents. It is clear from these studies that the photolysis of **5d**–**5f** in fluid
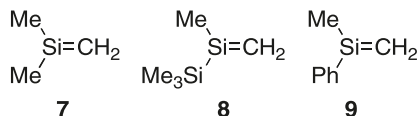
solution produces the corresponding silene derivatives in yields comparable to those of the corresponding silylenes and their co-product, Si$_2$Me$_6$, in all three cases. Thus, both reactive intermediates should in principle be detectable by laser flash photolysis methods, given an adequate appreciation of what to expect in the way of relative absorption intensities and reactivity patterns for the two species. The lowest energy (π,π*) absorption band in the UV–vis spectra of silenes of this general structure is relatively intense ($\varepsilon_{max} \geq 2 \times 10^4$ (mol/L)$^{-1}$ cm^{-1} (15), in contrast to the relatively weak ($\varepsilon_{max} \sim 10^3$ (mol/L)$^{-1}$ cm^{-1} (46)) lowest energy (n,p) absorption band in the UV–vis spectra of arylsilylenes. Given that the two types of products are formed in similar yields in all three cases, detection of the silene will clearly be a much easier task than detection of the silylene.

Our flash photolysis results for **5d**–**5f** are indeed consistent with the formation of two distinct transient products in all three cases. The dominant transient absorptions, which we assign to the silenes **6d**–**6f** based on comparisons of their absorption spectra and reactivities to those of the related an-

Chart 3.

$$\begin{array}{ccc} \underset{Me}{\overset{Me}{\diagdown}} Si=CH_2 & \underset{Me_3Si}{\overset{Me}{\diagdown}} Si=CH_2 & \underset{Ph}{\overset{Me}{\diagdown}} Si=CH_2 \\ \mathbf{7} & \mathbf{8} & \mathbf{9} \end{array}$$

alogues **6a–6c** (vide supra), are centered in the 440–460 nm spectral range and exhibit lifetimes of several hundred microseconds or greater; these are the species that were characterized in the earlier laser photolysis studies of **5d** (31, 32) and **5e** (33) in cyclohexane solution. Superimposed on these absorptions in hexane are those assignable to the corresponding silylenes, which are considerably shorter-lived and are quenched several orders of magnitude more rapidly than the 440–460 nm species by MeOH and Et$_3$SiH; in all three cases, the rate constants are close to the diffusion-controlled limit and are in good agreement with the values reported by us earlier for the reactions of SiMe$_2$ and SiPh$_2$ with the same substrates under similar conditions (34, 45). The presence of SiPh$_2$ in the end-of-pulse spectrum from **5e** is revealed by a relatively strong absorption band centered at λ_{max} = 290 nm, which is due to the $S_0 \rightarrow S_2$ transition of the silylene, and much weaker absorptions in the 480–530 nm range due to the $S_0 \rightarrow S_1$ transition, which we have shown is centered at λ_{max} = 515 nm in hexane at 25 °C (34). Similar short-lived absorptions (λ_{max} ~ 270, 510 nm) are observed in the end-of-pulse spectrum from laser photolysis of **5d**, superimposed on the much stronger absorptions of the long-lived transient coproduct (i.e., silene **6d**). The spectrum of this short-lived species is again quite similar to the low temperature matrix spectrum from **5d** (40), consistent with it being due to the corresponding silylene, SiMePh. With **5f**, on the other hand, the only short-lived absorptions detectable in the end-of-pulse spectrum are centered at λ_{max} ~ 290 nm, and the long wavelength absorption band expected for Si(Ph)SiMe$_3$ on the basis of its low temperature spectrum (44) could not be detected. This is very likely due simply to the lower sensitivity of our instrument at wavelengths above 600 nm coupled with the much lower extinction coefficient of the absorption compared to that at 290 nm (see Fig. 3*a*). Assignment of the latter to Si(Ph)SiMe$_3$ is supported by the observation that it is quenched by MeOH and Et$_3$SiH with rate constants similar to those measured for the other two silylenes.

The assignment of the dominant, long-lived absorptions to the corresponding silenes **6d–6f** is based on comparisons of their spectra and reactivities to those of the related analogues **6a–6c** (16, 17), coupled with a knowledge of the effects of methyl-, phenyl- and trimethylsilyl-substitution on the UV–vis spectra and reactivity of the "simple" silene derivatives **7–9** (Chart 3) and **3** (3, 13, 47–49). The difference in the absorption maxima of silenes **6d** (λ_{max} = 440 nm) and **6e** (λ_{max} = 460 nm) is consistent with the trend expected from consideration of the spectra of **6a–6c**, which exhibit a regular red-shift in λ_{max} as the methyl groups in **6a** (λ_{max} = 425 nm) are replaced with first one phenyl substituent (i.e., **6b**; λ_{max} = 460 nm) and then a second (i.e., **6c**; λ_{max} = 490 nm) (16). As has also been observed for **6a–6c** (16), there is no change in the positions of the absorption maxima of **6d–6f** upon changing the solvent from hexane to MeCN.

Scheme 2.
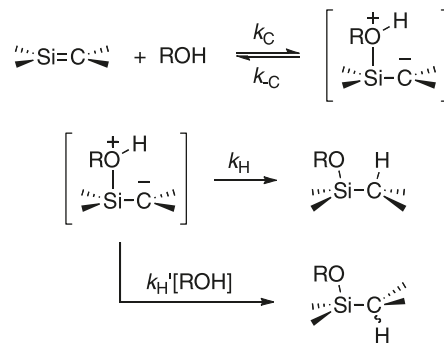
Similarly, the relative reactivities of **6d** and **6e** toward MeOH, AcOH, acetone, CCl$_4$, and O$_2$, with **6d** exhibiting modestly higher reactivity than **6e** in every case, are quite similar to the differences between the rate constants for reaction of **6a** and **6b** with the same six substrates, as well as to the corresponding differences between **6b** and **6c** (16, 17) (see Table 1). Substitution of a methyl substituent with trimethylsilyl at the silenic Si-atom is known to cause a somewhat smaller red-shift in the UV–vis spectra of silenes compared to phenyl-for-methyl substitution (cf. **7** (λ_{max} = 255 nm) (48), **8** (λ_{max} = 285 nm) (13), and **9** (λ_{max} = 315 nm) (49)), but results in substantially larger reductions in reactivity toward MeOH addition (cf. **7** (k_1 = 4.9 × 10^9 (mol/L)$^{-1}$ s^{-1}) (48), **8** (k_1 = 1.8 × 10^8 (mol/L)$^{-1}$ s^{-1}) (13), and **9** (k_1 = 3.2 × 10^9 (mol/L)$^{-1}$ s^{-1}) (49)). These trends lead to the prediction that compared to the series **6a–6c**, there should be a smaller red-shift in λ_{max} as one proceeds through the series **6a**, **6d**, and **6f**, accompanied by a much larger reduction in reactivity towards MeOH. Clearly, the results are in excellent agreement with this prediction. It can be concluded that the UV–vis spectra and reactivity exhibited by **6d–6f** follow trends that are not only internally consistent, but are consistent as well with those exhibited by **6a–6c** given the known effects of methyl-, phenyl-, and trimethylsilyl-substitution at silicon on the spectra and reactivity of other transient silene derivatives.

Comparison of the kinetic data for the two groups of compounds **6a/6d/6f** and **6c/6e/6f** allows a more detailed assessment of the effects of sequential trimethylsilyl substitution on the kinetics of the six silene-substrate reactions that have been studied in this work. In general, increasing TMS substitution in both series of compounds leads to a reduction in the rate constant for all six of these reactions, which is consistent with previously established trends for other silene derivatives (8, 50). However, the effect varies tremendously with the specific reaction type. For example, the sequential decrease in the rate constants for quenching by CCl$_4$ and O$_2$ with increasing TMS substitution in the two series of compounds is relatively small and more or less additive, while for quenching by acetone and DMB the introduction of the first TMS group results in a substantially larger reduction in reactivity than the introduction of the second TMS group. Interestingly, the opposite is true for quenching by MeOH and AcOH.

Of the six reactions studied, that with MeOH exhibits the largest substituent effect on the reaction kinetics. The mech-
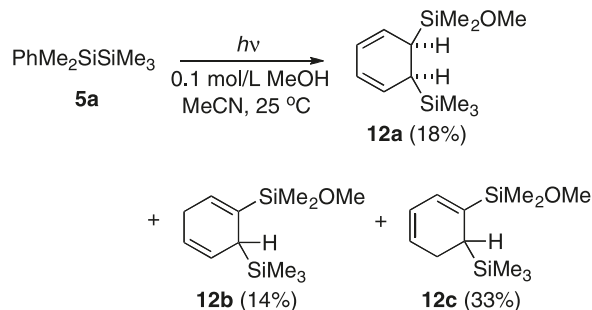
Scheme 3.

Scheme 4.
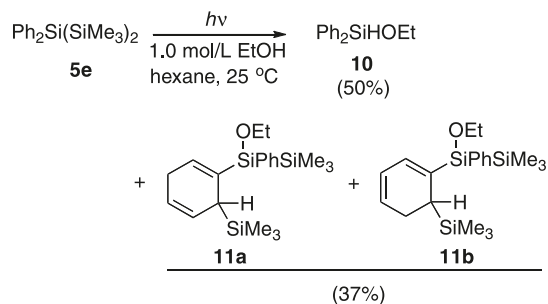
anism has been shown to involve initial, reversible nucleophilic attack at silicon to form a zwitterionic complex that proceeds to product via rate-controlling proton transfer from oxygen to the silenic carbon, the latter by competing unimolecular and catalytic pathways (Scheme 2) (10, 15, 17, 47). While this results in overall 1,2-addition in simple (nonconjugated) silenes, three regioisomers corresponding to 1,2-, 1,4-, and 1,6-addition are possible in the reaction of silenes of the type considered here, where the Si=C bond forms the terminus of a 1-silahexatrienyl system. The 1,4- and 1,6-addition products normally dominate the product mixtures from silenes of this type (51); this is exemplified by the results of Kira and co-workers (24, 25) for the photolysis of **5e** in hexane containing 1.0 mol/L ethanol, which yields ethoxydiphenylsilane (**10**; 50%; from trapping of SiPh$_2$) and the 1-silahexatriene-derived products **11a** and **11b** in a combined yield of 37% at 25 °C (Scheme 3). The corresponding 1,2-addition product has been reported in only one instance that we are aware of, from reaction of silene **6a** (generated by photolysis of **5a**) with MeOH (17). The product distribution obtained from reaction of silene **6a** with MeOH (Scheme 4) depends on the alcohol concentration, with reasonable yields of the 1,2-addition product (**12a**) being obtained only at very low alcohol concentrations (17). The 1,4- and 1,6-addition products (**12b** and **12c**, respectively) dominate the reaction mixture at higher alcohol concentrations, conditions that are typical of most of the published studies of the chemistry of silenes of this type. It can thus be concluded that these two regioisomers arise from the catalytic H-transfer pathway for decomposition of the initially formed silene-alcohol complex, while the 1,2-addition product results from the unimolecular H-transfer pathway (17).

The competition between unimolecular and catalytic intracomplex proton transfer is revealed in kinetic experiments by a quadratic dependence of the silene decay rate constant on alcohol concentration, since the catalyst for the latter pathway is a second molecule of the alcohol (see Scheme 2) (10, 15, 17). A variety of mechanisms are possible for the catalysis. With silenes such as **6a–6c** in polar solvents, the evidence suggests that it proceeds via a deprotonation-protonation sequence (17), favoring the formation of 1,4- and 1,6-adducts, as mentioned above. In principle, the process could alternatively proceed via a protonation-deprotonation sequence leading to predominant trans-addition (10) or via a concerted "proton-shuttling" mechanism in which the second molecule of alcohol acts si-

multaneously as acid and base. The transition state for this latter process is envisioned as being similar to that involved in the concerted reaction of the Si=C bond with the hydrogen-bonded dimer of the alcohol, as was proposed recently for the addition of MeOH to silene **2** in hexane solution (8) and should result in overall syn-addition. In any event, whether or not the predicted quadratic dependence of the silene decay rate constant (k_{decay}) on alcohol concentration can actually be observed with a given silene depends on the magnitude of the overall *second*-order rate constant and the maximum time resolution of the kinetic method. Strongly electrophilic silenes such as **3** and **9** (for which $k_1 \sim 10^9$ (mol/L)$^{-1}$ s^{-1} in MeCN) show only the first-order (in alcohol) kinetic component, because it is so fast that the lifetime of the silene becomes too short to be detected on the nanosecond time scale at the higher alcohol concentrations necessary for the second-order component (k_2) to become kinetically significant (47, 49). Moderately reactive silenes (such as **6a–6c**, for which $k_1 \leq 3 \times 10^8$ (mol/L)$^{-1}$ s^{-1} in MeCN) typically show both the first- and second-order components (3). Only the second-order component is observed with **6d** and **6e** (see Fig. 7a), indicating that the overall second-order reaction pathway is slowed so dramatically relative to that with **6a–6c** that it cannot be detected at all; the *only* kinetically significant mechanism for reaction of MeOH with these silenes involves two molecules of the alcohol in the transition state for the rate controlling step, and overall third order reaction kinetics. The rate constant for this process is more than 500 times slower than in **6a–6c**, reflecting a substantial reduction in electrophilicity due to the introduction of the TMS substituent at the silenic silicon atom. Silene **6f**, which bears *two* TMS-substituents at silicon, is so weakly electrophilic that its lifetime in MeCN is unaffected by addition of up to 2 mol/L MeOH, and it remains remarkably long-lived even in neat MeOH solution. There is not even a shift in the absorption maximum in the alcohol solvent relative to that in hexane or MeCN, which provides a further indication of the extremely low degree of electrophilicity of this silene derivative. The absorption spectra of all three derivatives are identical in THF and MeCN solution, as is also true of silenes **6b** and **6c**; of this series of silenes only **6a** exhibits a blue-shift of its absorption maximum in THF relative to its value in MeCN, due to complexation with the ether solvent (16). Silene **6f** is estimated to be roughly two orders of magnitude more reactive toward MeOH addition than the Apeloig silene **2**, from comparison of the lifetimes of the two species in MeOH (τ_{6f} =
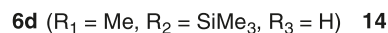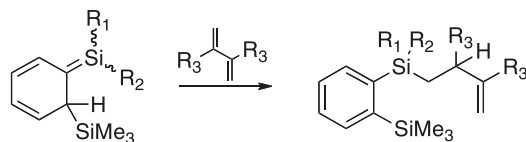
Scheme 5.
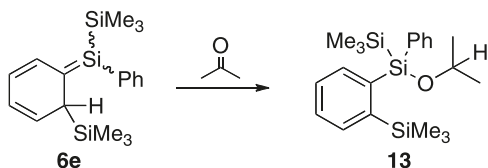
38 µs) or 9:1 *v/v* MeOH:THF ($\tau_2 \sim 14$ ms (8)) at 25 °C. This could be the simple result of the pronounced differences in steric bulk of the adamantylidene and cyclohexadienylidene substituents at the silenic carbon in the two silenes.
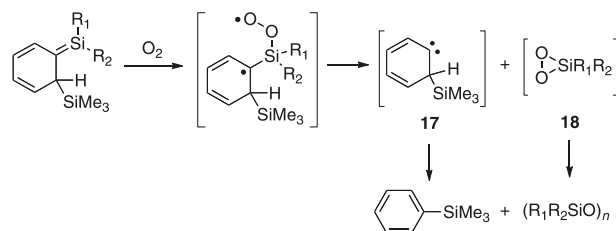
More moderate variations in rate constants are observed for quenching of the six silenes by acetone, AcOH, and DMB, which proceeds with clean overall second order kinetics in all cases. The major product of the reaction of silene **6e** with acetone is the silyl enol ether derived from formal ene-addition of the ketone C=O bond across the 1-silaallyl moiety of the silene (**13**; Scheme 5) (37); the analogous compounds are also the major products of the reactions of **6a–6c** with this ketone, accompanied by minor amounts of the siloxetanes derived from formal [2+2] cycloaddition (16). The formation of the latter products from silenes of this type is most likely general, but as they are rather sensitive to thermal and (or) hydrolytic decomposition, they have been detected in only a few instances (16, 38). The reaction is thought to proceed via a two-step mechanism initiated by formation of a biradical or zwitterionic intermediate that collapses to products via competing ring-closure and intramolecular H-migration (16, 38). The course of the reactions of silenes of this type with AcOH has not been fully established; the product mixture resulting from reaction of AcOH with silene **6a** proved to be intractable in earlier studies, leading to a complex mixture of at least eight products in MeCN solution (17). However, with simpler silenes such as **3** the reaction is known to proceed via formal 1,2-addition of AcOH across the Si=C bond (47). The mechanism is presumably analogous to an ene-addition, involving bonding of the carbonyl oxygen to silicon and transfer of the hydroxyl proton to carbon. The reactions of 1,3-butadiene with **6d** and DMB with **6e** and **6f** afford the corresponding ene-addition products (**14–16**; Scheme 6) (23, 26, 37), in identical fashion to the reaction of aliphatic dienes with other (phenyldisilane-derived) 1-silahexatrienes, such as **6a–6c** (16, 52). It is interesting to note that the rate constants for reaction of **6a/6d/6f** and **6c/6e/6f** with DMB follow similar trends as those for reaction with acetone (see Table 1), suggesting that for these silenes, Si=C bond polarity provides a similar driving force in both reactions.

The reactions of silenes of this type with O_2 and CCl_4 are unique in that they proceed much faster than is the case with simpler silene derivatives (3). This suggests that the substitution pattern at the silenic carbon is the main factor controlling the rates of these reactions, with substitution at the silenic Si atom playing only a secondary role. Accordingly, the span in reactivity throughout the present series of compounds toward these two substrates is relatively small, varying by a factor of less than 100 throughout the series (see Table 1); with **6d–6f**, these are the fastest reactions that these silenes undergo.

Scheme 6.

6d (R$_1$ = Me, R$_2$ = SiMe$_3$, R$_3$ = H)   **14**
6e (R$_1$ = Ph, R$_2$ = SiMe$_3$, R$_3$ = Me)   **15**
6f   (R$_1$ = R$_2$ = SiMe$_3$, R$_3$ = Me)   **16**

Scheme 7.

The reaction with O_2 is thought to proceed via rate-determining attack of the substrate at the silenic Si atom to yield the corresponding triplet 1,4-biradical, which in the present series of compounds enjoys significant resonance stabilization owing to the fact that the C-terminus is part of a cyclohexadienyl system (16). In the cases of **6a** and **6c**, the final products of the reaction are phenyltrimethylsilane and the corresponding silanone oligomers, $(Me_2SiO)_n$ from **6a** and $(Ph_2SiO)_n$ from **6c**, which have been proposed to be formed from carbene **17** and dioxasilirane **18**, respectively, produced by cleavage of the 1,4-biradical (Scheme 7) (16).

The product mixtures resulting from the reaction of silenes of this type with CCl_4 have not been fully characterized; we reported previously that photolysis of **5a** and **5c** in cyclohexane-d_{12} containing 0.03 mol/L CCl_4 leads to complex mixtures of products that include the chlorosilanes derived formally from Si–Si bond homolysis, and hexachloroethane (16). A reinvestigation of the photolysis of **5a** in the presence of CCl_4 under similar conditions to those used in our earlier study (0.03 mol/L **5a**; 0.03 mol/L CCl_4), and monitoring the course of the photolysis at low (ca. 3%–12%) conversions by (600 MHz) ^{1}H NMR spectroscopy, allowed quantification of the chemical yields of PhMe$_2$SiCl (50%) and Me$_3$SiCl (26%) relative to consumed **5a**; chloroform (as CHCl$_3$; 14%) was also identified in the mixture. The spectra also showed evidence for the formation of at least one additional aromatic product, and a series of resonances in the δ 2.7–4 and δ 5.7–6.4 regions that are characteristic of 1,3- and 1,4-cyclohexadiene derivatives (16, 17), in significant yields. On the basis of these results, we suggest that the reaction of **6a** with CCl_4 most likely proceeds via Cl atom abstraction to yield cyclohexadienyl radical **19** and the trichloromethyl radical (Scheme 8). The formation of PhMe$_2$SiCl is then accounted for by β-scission of radical **19**, while CHCl$_3$ and the unidentified aromatic and cyclohexadiene products are the products expected from coupling and disproportionation processes involving **19** and

Scheme 8.
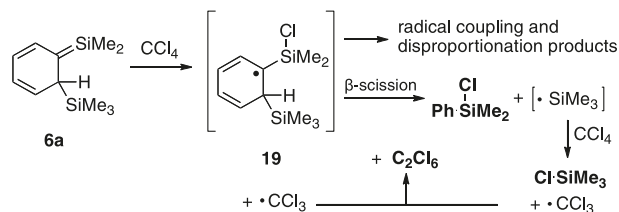
trichloromethyl and trimethylsilyl radicals, the latter being produced as the coproduct of the β-scission process in **19**.

It has been suggested that the reaction is likely initiated by electron transfer, based on the facts that quenching of **6a–6c** by CCl_4 is significantly faster in MeCN than in hydrocarbon solvents and more than 100 times faster than quenching by chloroform (16). The very modest variation in rate constant throughout the present series of compounds is probably also consistent with this notion, to the extent that varying combinations of methyl-, phenyl-, and trimethylsilyl-substitution at the silenic silicon would be expected to have relatively small effects on the oxidation potential of the 1-silahexatrienyl moiety that is common to all six of these silenes.

Finally, it is interesting to note that the UV–vis spectra recorded after photolysis of **5d–5f** in 3-MP matrixes at 78 K differ significantly from the time-resolved spectra obtained by flash photolysis in fluid solution at room temperature (see Figs. 1–3 and ref. (33)). This is consistent with a marked difference in the temperature and (or) medium dependences of the quantum yields for formation of the corresponding silylenes and silenes from photolysis of these compounds, with silene formation being suppressed almost entirely when the three compounds are photolysed in solid matrixes at low temperature.

Summary and conclusions

Laser flash photolysis of the well-known silylene precursors **5d–5f** in hexane solution leads to strong, long-lived transient absorptions due to the corresponding silene derivatives **6d–6f**, superimposed on the very weak, much shorter-lived absorptions due to the silylenes SiMePh (from **5d**), $SiPh_2$ (from **5e**), and $Si(Ph)SiMe_3$ (from **5f**). The UV–vis spectra of the silylenes in hexane solution can be extracted from the raw transient spectra by selective quenching with Et_3SiH, which reacts several orders of magnitude more rapidly with the silylenes than with the corresponding silenes. The resulting spectra are quite similar to those recorded in a 3-methylpentane matrix at 78 K, where photolysis of **5d–5f** affords the silylenes with high selectivity. In solution at room temperature, photolysis of the three compounds affords the corresponding silenes and silylenes in nearly equal yields.

Along with the related, phenyldisilane-derived silene derivatives **6a–6c**, the three silenes studied in the present work form a contiguous series of silenes bearing the six possible combinations of methyl-, phenyl-, and trimethylsilyl-substituents at the silenic silicon atom. The UV–vis spectra of the six silenes vary in a rational way with substitution, as do the absolute rate constants for their reactions with metha-

nol (MeOH), acetic acid (AcOH), acetone, 2,3-dimethyl-1,3-butadiene (DMB), molecular oxygen, and carbon tetrachloride in hexane or MeCN solution. The results allow the first systematic, quantitative study of the well-known stabilizing effects of trimethylsilyl substitution at the silicon atom in silenes, applied to a selection of different reaction types. These include the nucleophilic addition of alcohols, the formal ene-addition reactions of carboxylic acids, ketones, and dienes, and the radical-like reactions with oxygen and CCl_4. All are slowed significantly by trimethylsilyl substitition at the silenic silicon atom, underlining the importance of Si=C bond polarity as a common, general driving force in the reactions of silenes.

Experimental

Compounds **5a** and **5d–5f** were prepared by the published methods (26, 53–55) and purified by vacuum distillation followed by column chromatography on silica gel using hexanes as eluant. Acetone (Caledon Reagent) was used as received from the supplier. Methanol (Baker Photrex) and 2,3-dimethyl-1,3-butadiene (Sigma-Aldrich) were distilled. Carbon tetrachloride (Sigma-Aldrich) was purified by distillation over P_2O_5 and passed through a short silica gel column. Glacial acetic acid (Sigma-Aldrich), acetonitrile (Caledon HPLC), and 3-methylpentane (Sigma-Aldrich spectrophotometric grade) were used as received from the suppliers. Triethylsilane (Sigma-Aldrich) was distilled from lithium aluminum hydride. Hexanes (EMD OmniSolv) and tetrahydrofuran (Caledon Reagent) were dried by passage through activated alumina under nitrogen using a Solv-Tek solvent purification system (Solv-Tek, Inc). Deuterated solvents were used as received from Cambridge Isotope Laboratories.

Laser flash photolysis experiments employed the pulses from a Lambda Physik Compex 120 excimer laser filled with $F_2/Kr/Ne$ mixtures (248 nm; 25 ns; 90–120 mJ/pulse), and a Luzchem Research mLFP-111 laser flash photolysis system, modified as described previously (56). Solutions were prepared at concentrations (ca. 10^{-4} mol/L) such that the absorbance at the excitation wavelength (248 nm) was ca. 0.7, and were flowed through a 7 × 7 mm Suprasil flow cell from calibrated 100 or 250 mL reservoirs, fitted with a glass frit to allow bubbling of argon gas through the solution for at least 30 min prior to and then throughout the duration of each experiment, using a Masterflex™ 77390 peristaltic pump fitted with Teflon tubing (Cole-Parmer Instrument Co.). The sample cell and transfer lines were dried before use in a vacuum oven at 65–85 °C, while the reservoir was flame-dried and allowed to cool under an argon atmosphere. Reagents were added directly to the reservoir by microliter syringe as aliquots of standard solutions. Rate constants were calculated by linear least-squares analysis of decay rate-concentration data consisting of at least 10 points for all substrates except oxygen. For the latter, they were calculated from k_{decay} values in Ar-, air- and O_2-saturated solution, with use of neutral density filters to achieve reasonably clean pseudo first order kinetics in Ar-saturated solution. The errors in the absolute rate constants are quoted as twice the standard error obtained from the least-squares analyses.

Low temperature UV–vis spectroscopic experiments employed 2 cm × 1 cm × 1 cm cuvettes constructed from Suprasil quartz tubing (Vitro Dynamics, Inc.) and an Oxford Optistat™ liquid nitrogen cryostat equipped with an Oxford ITC601 temperature controller. Samples were irradiated in a Rayonet Photochemical Reactor (Southern New England Ultraviolet Company) fitted with 12 RPR-2537 lamps.

Steady state photolysis of a 0.031 mol/L solution of **5a** in C_6D_{12} containing CCl_4 (0.03 mol/L) and CH_2Cl_2 (0.005 mol/L; internal standard) was carried out in a quartz NMR tube, after deoxygenating the solution with a fine stream of argon and sealing the tube with a rubber septum. The photolysis was monitored at periodic time intervals by 600 MHz ^{1}H NMR spectroscopy (Bruker AV600), and chemical yields were determined from the slopes of concentration versus time plots, constructed by integration of the peaks due to **5a** and those products that could be specifically identified in the photolysate ($PhMe_2SiCl$, Me_3SiCl, and $CHCl_3$) by spiking the mixture with authentic samples. Representative NMR spectra and concentration versus time plots are given in the Supplementary Data.[2]

Acknowledgement

References

1. G. Raabe, J. Michl, S. Patai, and Z. Rappoport. *In* The chemistry of organic silicon compounds. John Wiley & Sons, New York. 1989. pp. 1015–1142.
2. A.G. Brook and M.A. Brook. Adv. Organomet. Chem. **39**, 71 (1996).
3. T.L. Morkin, T.R. Owens, W.J. Leigh, Z. Rappoport, and Y. Apeloig. *In* The Chemistry of organic silicon compounds. Vol. 3. *Edited by* Z. Rappoport. John Wiley and Sons, New York. 2001. pp. 949–1026.
4. H. Ottosson and P.G. Steel. Chem. Eur. J. **12**, 1576 (2006).
5. A.G. Brook, F. Abdesaken, B. Gutekunst, G. Gutekunst, and R.K. Kallury. Chem. Commun. 191 (1981).
6. D. Bravo-Zhivotovskii, V. Braude, A. Stanger, M. Kapon, and Y. Apeloig. Organometallics, **11**, 2326 (1992).
7. S. Zhang, R.T. Conlin, P.F. McGarry, and J.C. Scaiano. Organometallics, **11**, 2317 (1992).
8. W.J. Leigh, T.R. Owens, M. Bendikov, S.S. Zade, and Y. Apeloig. J. Am. Chem. Soc. **128**, 10772 (2006).
9. A.G. Brook, J.W. Harris, J. Lennon, and M. El Sheikh. J. Am. Chem. Soc. **101**, 83 (1979).
10. M. Kira, T. Maruyama, and H. Sakurai. J. Am. Chem. Soc. **113**, 3986 (1991).
11. H. Sakurai, Z. Rappoport, and Y. Apeloig. *In* The chemistry of organic silicon compounds. John Wiley and Sons, Ltd., New York. 1998. pp. 827–855.
12. K.K. Milnes and K.M. Baines. Organometallics, **26**, 2392 (2007).
13. W.J. Leigh, R. Boukherroub, and C. Kerst. J. Am. Chem. Soc. **120**, 9504 (1998).
14. W.J. Leigh, C. Kerst, R. Boukherroub, T.L. Morkin, S. Jenkins, K. Sung, and T.T. Tidwell. J. Am. Chem. Soc. **121**, 4744 (1999).
15. G.W. Sluggett and W.J. Leigh. J. Am. Chem. Soc. **114**, 1195 (1992).
16. W.J. Leigh and G.W. Sluggett. Organometallics, **13**, 269 (1994).
17. W.J. Leigh and G.W. Sluggett. J. Am. Chem. Soc. **116**, 10468 (1994).
18. M. Ishikawa and M. Kumada. Adv. Organomet. Chem. **19**, 51 (1981).
19. P.P. Gaspar, M. Jones, Jr., and R.A. Moss. *In* Reactive intermediates. Vol. 3. John Wiley & Sons, New York. 1985. pp. 333–427.
20. H. Shizuka and H. Hiratsuka. Res. Chem. Intermed. **18**, 131 (1992).
21. M.G. Steinmetz. Chem. Rev. **95**, 1527 (1995).
22. P.P. Gaspar, R. West, Z. Rappoport, and Y. Apeloig. *In* The chemistry of organic silicon compounds. Vol. 2. *Edited by* Z. Rappoport. John Wiley and Sons, New York. 1998. pp. 2463–2568.
23. M. Ishikawa, K.I. Nakagawa, R. Enokida, and M. Kumada. J. Organomet. Chem. **201**, 151 (1980).
24. M. Kira, T. Miyazawa, S.Y. Koshihara, Y. Segawa, and H. Sakurai. Chem. Lett. **1995**, 3 (1995).
25. T. Miyazawa, S.Y. Koshihara, C. Liu, H. Sakurai, and M. Kira. J. Am. Chem. Soc. **121**, 3651 (1999).
26. M. Ishikawa, K.I. Nakagawa, and M. Kumada. J. Organomet. Chem. **178**, 105 (1979).
27. R. Nakao, K. Oka, S. Irie, T. Dohmaru, Y. Abe, and T. Horii. J. Chem. Soc. Perkin Trans. 2, **1991**, 755 (1991).
28. M. Ishikawa, S. Katayama, and M. Kumada. J. Organomet. Chem. **248**, 251 (1983).
29. M. Ishikawa, K.I. Nakagawa, M. Ishiguro, F. Ohi, and M. Kumada. J. Organomet. Chem. **152**, 155 (1978).
30. M. Ishikawa, K. Nakagawa, and M. Kumada. J. Organomet. Chem. **135**, C45 (1977).
31. P.P. Gaspar, D. Holten, S. Konieczny, and J.Y. Corey. Acc. Chem. Res. **20**, 329 (1987).
32. P.P. Gaspar, B.H. Boo, S. Chari, A.K. Ghosh, D. Holten, C. Kirmaier, and S. Konieczny. Chem. Phys. Lett. **105**, 153 (1984).
33. S. Konieczny, S.J. Jacobs, J.K. Braddock Wilking, and P.P. Gaspar. J. Organomet. Chem. **341**, C17 (1988).
34. A.G. Moiseev and W.J. Leigh. Organometallics, **26**, 6268 (2007).
35. A.G. Brook, Z. Rappoport, and Y. Apeloig. *In* The chemistry of organic silicon compounds. John Wiley and Sons, New York. 1998. pp. 1233–1310.
36. M. Ishikawa and H. Sakamoto. J. Organomet. Chem. **414**, 1 (1991).
37. K.L. Bobbitt and P.P. Gaspar. J. Organomet. Chem. **499**, 17 (1995).
38. N.P. Toltl and W.J. Leigh. Organometallics, **15**, 2554 (1996).
39. C.J. Bradaric and W.J. Leigh. Organometallics, **17**, 645 (1998).
40. M.J. Michalczyk, M.J. Fink, D.J. De Young, C.W. Carlson, K.M. Welsh, R. West, and J. Michl. Silicon, Germanium, Tin Lead Compd. **9**, 75 (1986).
41. A.G. Moiseev and W.J. Leigh. Organometallics, **26**, 6277 (2007).
42. J.A. Hawari, M. Lesage, D. Griller, and W.P. Weber. Organometallics, **6**, 880 (1987).
43. A. Sekiguchi, I. Maruki, and H. Sakurai. J. Am. Chem. Soc. **115**, 11460 (1993).

44. S.G. Bott, P. Marshall, P.E. Wagenseller, Y. Wang, and R.T. Conlin. J. Organomet. Chem. **499**, 11 (1995).
45. A.G. Moiseev and W.J. Leigh. J. Am. Chem. Soc. **128**, 14442 (2006).
46. R.T. Conlin, J.C. Netto-Ferreira, S. Zhang, and J.C. Scaiano. Organometallics, **9**, 1332 (1990).
47. W.J. Leigh, C.J. Bradaric, C. Kerst, and J.H. Banisch. Organometallics, **15**, 2246 (1996).
48. C. Kerst, R. Boukherroub, and W.J. Leigh. J. Photochem. Photobiol. A, **110**, 243 (1997).
49. W.J. Leigh, R. Boukherroub, C.J. Bradaric, C.C. Cserti, and J.M. Schmeisser. Can. J. Chem. **77**, 1136 (1999).
50. T.R. Owens, J. Grinyer, and W.J. Leigh. Organometallics, **24**, 2307 (2005).
51. M. Ishikawa, T. Fuchikami, and M. Kumada. J. Organomet. Chem. **118**, 155 (1976).
52. M. Ishikawa, T. Fuchikami, and M. Kumada. J. Organomet. Chem. **118**, 139 (1976).
53. V.J. Tortorelli, M. Jones, Jr., S. Wu, and Z. Li. Organometallics, **2**, 759 (1983).
54. M. Kumada, M. Ishikawa, and S. Maeda. J. Organomet. Chem. **2**, 478 (1964).
55. H. Gilman, D.J. Peterson, and D. Wittenberg. Chem. Ind. (London), 1479 (1958).
56. K. Nishiyama, M. Oba, H. Takagi, I. Fujii, N. Hirayama, Narisu, H. Horiuchi, T. Okutsu, and H. Hiratsuka. J. Organomet. Chem. **604**, 20 (2000).